

# The Effect of Compression Induced Chorus Waves on 10s to 100s eV Electron Precipitation

A. J. Halford<sup>1</sup>, K. Garcia-Sage<sup>1</sup>, I. R. Mann<sup>2</sup>, D. L. Turner<sup>3</sup>, A. W.  
Breneman<sup>1</sup>

<sup>1</sup>NASA Goddard Space Flight Center, College Park, MD, USA

<sup>2</sup>Department of Physics, University of Alberta, Edmonton, Alberta, Canada

<sup>3</sup>Johns Hopkins University Applied Physics Laboratory, Laurel, MD, United States

## Key Points:

- Upper Band Chorus waves can have a minimum resonant energy in the 10s eV energy range.
- Changes in the minimum resonant energy can change the cut off for what lower energy particles will be lost.
- The lower energy cut off can be observed in the Van Allen Probes HOPE data.

---

Corresponding author: A.J. Halford, [alex.a.j.halford@nasa.gov](mailto:alex.a.j.halford@nasa.gov)

## Abstract

On 7 January 2014, a solar storm erupted, which eventually compressed the Earth's magnetosphere leading to the generation of chorus waves. These waves enhanced local wave-particle interactions and led to the precipitation of electrons from 10s eV to 100s keV. This paper shows observations of a low energy cutoff in the precipitation spectrum from Van Allen Probe B Helium Oxygen Proton Electron (HOPE) measurements. This low energy cutoff is well replicated by the predicted loss calculated from pitch angle diffusion coefficients from wave and plasma observations on Probe B. To our knowledge, this is the first time a single spacecraft has been used to demonstrate an accurate theoretical prediction for chorus wave-induced precipitation and its low energy cutoff. The specific properties of the precipitating soft electron spectrum have implications for ionospheric activity, with the lowest energies mainly contributing to thermospheric and ionospheric upwelling, which influences satellite drag and ionospheric outflow.

## Plain Language Summary

On 7 January 2014, a large storm erupted from the Sun. This storm encountered the Earth and compressed the magnetosphere a few days later. The compression of the magnetosphere led to the creation of chorus waves, a wave-type known to interact only with electrons with specific energies. In this case, the waves interacted with electrons in the magnetosphere's outer radiation belt. They caused the loss of electrons from 10s eV to 100s keV into the ionosphere and upper atmosphere. This paper uses theory to determine which energies we expect will interact with the observed chorus wave. We use the HOPE instrument from the Van Allen Probes to see if our predictions are correct. We care about these processes because the loss of these electrons can affect ionospheric activity.

## 1 Introduction

Upper band chorus waves have a minimum resonant energy typically found in the energy range of 10s - 100s eV and are known to lead to the loss of these electrons to the upper atmosphere (e.g., Meredith et al., 2003; Summers et al., 2007; Ni et al., 2008; Z. Su et al., 2010; Li et al., 2011). The precipitation of electrons just above this cutoff energy into the upper atmosphere may help drive both neutral thermospheric upwelling, which influences satellite drag (e.g., Clemmons et al., 2008; Zhang et al., 2012; Deng et al., 2011), and ion upflow that may lead to outflow (e.g., Y.-J. Su et al., 1999; Zeng & Horwitz, 2007; Redmon et al., 2014, and references within these papers). Seo et al. (1997) showed correlations between up-flows and electron precipitation for energies less than 80 eV observed by the DE 2 satellite at 850 - 950 km altitude. (Redmon et al., 2014) demonstrated using single field-line modelling that 50 eV precipitation is more effective than higher energies at producing  $O^+$  upflow at 850 km altitude. The effective precipitation energies for thermospheric upwelling are only slightly higher, with results from Clemmons et al. (2008) and Zhang et al. (2012) indicating that precipitation energies of 100 eV and 200 eV act to increase thermospheric density at 400 km. The upflow ion populations provide the source population for ion outflow into the magnetosphere. The outflow, in turn, can affect reconnection rates, sawtooth events, electromagnetic ion cyclotron wave growth, and other geomagnetic processes (e.g., Baker et al., 1982; Daglis et al., 1999; Ouellette et al., 2013; Garcia-Sage et al., 2015; Halford, Fraser, et al., 2016, and references within these papers). Indeed, Gkioulidou et al. (2019) found evidence of ion outflow directly into the inner magnetosphere, leading to the possible formation of the  $O^+$  torus just outside of the plasmopause (e.g., Nosé et al., 2015, and references therein). Ion outflow may require the presence of multiple energization processes working in concert (e.g., Zeng & Horwitz, 2007) where the chorus wave-induced precipitation presented here indicates one potential contributing mechanism.

On 7 January 2014, a coronal mass ejection (CME) erupted off of the Sun, and the edge of the ICME arrived at the Earth on 9 January at 20:10:30 UT (e.g., Möstl et al., 2015; Mays et al., 2015; Halford et al., 2015; Halford, McGregor, et al., 2016). The interplanetary magnetic field (IMF)  $B_z$  component was positive or near zero for the majority of the event (Figure 2 in Halford et al., 2015), and therefore did not trigger a geomagnetic storm or substorm in the Earth’s magnetosphere (Mays et al., 2015; Halford et al., 2015). However, this encounter did significantly compress the magnetopause inwards by 1 Earth radii ( $R_E$ ) as determined by Halford et al. (2015). Three Balloon Array for Radiation belt Relativistic Electron Loss (BARREL) payloads (2K, 2L, and 2X) X-ray detectors inferred loss of 10s - 100s keV radiation belt electrons. They mapped to the dayside inner magnetosphere and were near conjugate to both of the Van Allen Probes (see Figure 4 Halford et al., 2015). Halford et al. (2015) discussed the loss of 100s keV electrons from the magnetopause compression and observed chorus, hiss, and electromagnetic ion cyclotron waves. The loss of these particles due to the compression described in detail in Halford et al. (2015) is summarised in the following steps: First, compression-driven ExB drift motion pushed particles inward by approximately  $1 R_E$  within 2 minutes. This inward motion, assuming conservation of the first and second adiabatic invariants, increased the particles’ pitch angles, but also moved them into a region with a larger loss cone (e.g. Rae et al., 2018). As discussed in Halford et al. (2015), the amount of loss cone increase exceeded the increase in pitch angle, resulting in a loss of particles within  $0.5^\circ$  of the initial  $\sim 3^\circ$  loss cone. The chorus wave is then observed to grow and further interacts with the particles and pitch angle scatters them into the loss cone. While BARREL was limited in the energy range of electron precipitation that could be inferred, the observed wave was theoretically able to interact with energies in the 10s of eV range.

In this paper, we examine the effect of the upper band chorus on lower-energy electrons. The observed chorus wave on January 9th 2014 can precipitate electrons down to much lower energies of 10s of eV, Figure 1 (e.g., Z. Su et al., 2010; Li et al., 2011; Halford et al., 2015), well below the minimum energy threshold observable by BARREL, but within the observational range of the HOPE instrument. Although this event did not result in a geomagnetic storm or a significant change in the trapped population of the radiation belts, it has allowed for a close examination of the wave-particle dynamics which occur during geomagnetic compressions, and a comparison of the relative loss due to the triggered plasma waves and the large-scale electric field impulse. In this paper, we will focus on the expected and observed interactions between the chorus waves and the 10s to 100s of eV electrons at the location of Van Allen Probe B.

## 2 Data

The two Van Allen Probes satellites are in  $\sim 9$  hour near-equatorial elliptical orbits with an apogee near  $L = 6$  (Mauk et al., 2012). During the event considered here, Van Allen Probe B was at an L-value of approximately 5.8, an MLT value of 13.2, and a magnetic latitude of approximately 1 deg off the magnetic equator. As the event studied in this paper only lasted approximately 10 minutes, the satellite is relatively stationary. Each of the Van Allen Probe satellites were equipped with instruments allowing for observations of waves and particles across multiple orders of magnitude in amplitude and energy. For this study, we will use data from the Electric and Magnetic Fields Instrument Suite and Integrated Science (EMFISIS) wave instrument (Kletzing et al., 2013), as well as the Helium, Oxygen, Proton, and Electron (HOPE) mass spectrometer (Funsten et al., 2013) from the Energetic Particle Composition and Thermal Plasma Suite (ECT; (Spence et al., 2013)). The HOPE instrument covers an electron energy range of  $\sim 10$  eV - 50 keV.

### 3 Results

Using the observed wave and plasma characteristics given in Halford et al. (2015) we can solve for the minimum resonant energy,  $E_{min}$ , given in equation 16 in Summers et al. (2007) as

$$E_{min} = \left[ 1 - \frac{(v_{||})^2}{c^2} \right]^{-1/2} - 1. \quad (1)$$

where  $c$  is the speed of light and  $v_{||}$  is the particle's parallel velocity. The expected pitch angle diffusion ( $D_{\alpha,\alpha}$ ) can be written as

$$D_{\alpha,\alpha} = \frac{\pi\Omega_\sigma^2}{2\rho|\Omega_e|} \frac{1}{(E+1)^2} \sum_s \sum_j \frac{R(1 - \frac{x_j \cos\alpha}{y_j \beta})^2 |\delta x_j / \delta y_j|}{\delta x |(\beta \cos\alpha - \delta x_j / \delta y_j|} e^{-\left(\frac{x_j - x_m}{\delta x}\right)^2} \quad (2)$$

for specific energies as described in Summers et al. (2007) and given in equations 5 and 30 of their paper. Within equation 2  $E$  is the dimensionless particle kinetic energy  $E = (1 - v^2/c^2)^{-1/2} - 1$  where  $v$  is the particle's velocity,  $\beta = v/c$ ,  $\Omega_e$  is the non-relativistic electron gyro-frequency,  $\Omega_\sigma$  is the non-relativistic particle gyro-frequency,  $R$  is relative wave power,  $x = \omega/|\Omega_e|$ ,  $y = ck/|\Omega_e|$  where  $k$  is the wave number,  $x_m = \omega_m/|\Omega_e|$ , and  $\delta x = \delta\omega/|\Omega_e|$ . The particle species is  $j$  and  $s$  is the wave mode, 1 for R-mode waves.  $\delta x_j / \delta y_j$  is further defined in Summers et al. (2007) and is taken from the appropriate dispersion relation. We can then compare our estimates of the energy and pitch angle of the particles affected to the observations from the HOPE instrument on Van Allen Probe B.

In Halford et al. (2015)  $D_{\alpha,\alpha}$ s were calculated for electron energies of 10s - 100s of keV shown in their Figure 8. In this paper, we consider the wave-particle interactions for the low energy electrons (10 - 100s eV) where the minimum resonance energy is found. We calculate the  $D_{\alpha,\alpha}$  for a given HOPE energy channel and compare the expected results to the observed pitch angle distributions for the proper HOPE energy bin.

As the shock arrives, the plasmasphere is observed to move earthward of the satellite, and the chorus wave is observed at Van Allen Probe B as discussed and shown in Halford et al. (2015). As Van Allen Probe A stayed within the plasmasphere/plasmaplume, it did not observe a chorus wave but instead saw a Hiss wave as discussed in Halford et al. (2015). Figure 1 panel a) shows the observations of the chorus wave on Van Allen Probe B located at  $L \sim 5.8$ . As the wave was generated locally the wave was observed to be approximately normal with the magnetic field. The minimum resonant energy for a chorus wave depends greatly on the local plasma conditions and wave frequency (Summers et al., 2007; Z. Su et al., 2010). The average wave and plasma conditions throughout the duration of the wave used to calculate  $D_{\alpha,\alpha}$  from equation 2 are a wave amplitude of  $2.5 \times 10^{-2}$  nT, a background magnetic field of 167 nT, a cold plasma density of  $12 \text{ cm}^{-3}$ , a centre frequency of  $\sim 0.56\Omega_e$ , and a bandwidth of  $\sim 0.1\Omega_e$ . From Equation 1, these values lead to average minimum resonance energy from the chorus wave of  $\sim 26$  eV. However, it should be noted that the diffusion time scales for energies up to 40 eV are shorter than the observed duration of the wave. Thus we do not expect to observe any significant changes in the pitch angle distributions at these lowest energies as can be seen in Figure 1 panels b and c.

In panels b,d,f, and h both the expected local (solid line) and bounce averaged (dotted line) pitch angle diffusion coefficients are plotted for the HOPE energy bins centred around approximately 33 eV, 67 eV, 235 eV (which had the maximum values for both the bounced average and local  $D_{\alpha,\alpha}$ 's), and 660 eV respectively. The X-axis has a minimum value of approximately one over the length of time the chorus wave was observed. The pitch angle distributions for these energy channels are plotted in panels c, e, g, and i. The narrowing of the trapped population is observed and is consistent with the expected range of pitch angles affected by the observed chorus wave.

In Figure 2, we have plotted the normalised pitch angle distribution during three periods around the event. Panel a-d correspond to the energies plotted in Figure 1. The dashed lines in each of the panels represent the bounce averaged diffusion coefficients from the observed upper band chorus from Figure 1 for reference. The dark blue lines in each panel show the mean normalised pitch angle distribution before the compression event. As expected, the distributions are very isotropic. The green lines are the normalised pitch angle distributions during the period from the start of the compression until the start of the wave. Here we can see a small peak around  $90^\circ$  for all energies. This is consistent with the compression causing the particles' pitch angles to move closer to 90 degrees. The red lines show the mean pitch angle distribution during the period where the chorus wave is observed. The pitch angle distributions have become more peaked. They also show an energy dependence with the higher energy electron populations becoming more steeply peaked. The pitch angles within the 105 and 660 eV channels affected by the chorus wave appear to be more efficiently cleared out than those in the  $\sim 66$  eV channel, as shown in both Figures 1 and 2. This is likely because the bounced-averaged diffusion in both of these higher energy bins exceeds the local strong diffusion limit of  $\sim 10^{-4}$  while the bounce averaged diffusion for the 66 eV channel is below this limit (e.g., Shultz & Lanzerotti, 1974; Halford, 2012; Ni et al., 2008).

With this event, we can directly compare the different effects that the shock-induced electric field impulse and the chorus waves will have on the 10s to 100s eV particles. The electric field impulse will affect (and ultimately cause loss of) particles independent of energy and species. Specifically, particles of any energy or species within  $0.5^\circ$  of the loss cone are expected to be lost to the atmosphere. The adiabatic transport will move particles towards 90 degrees, but as shown in more detail in Halford et al. (2015) the expected change in a given pitch angle is less than  $2^\circ$ , and consequently not able to account for the dramatic narrowing of the distribution at the higher energies, e.g., 660 eV in panel i of Figure 1 (see also Rae et al., 2018). The chorus waves, on the other hand, will be selective in the energies and pitch angles of electrons they scatter.

## 4 Discussion

Electron precipitation at these low energies has been shown through both statistical studies and modelling to be effective for ion upflow. While secondary electron production will further enhance these low-energy electron populations (Khazanov et al., 2017), this study indicates that chorus waves lead to precipitation of soft electrons with a hard lower energy cutoff within or near the energy range of interest of upwelling and outflow, with the cutoff for this event at  $\sim 26$  eV. To our knowledge, this is the first observation of both the chorus waves and evidence of their minimum resonant energy cut off from in situ observations at the same satellite and at the same time. In this paper, we do not show the impact of the sharp low energy cut off for the precipitating energy spectrum, but we suggest that the effects of this cutoff should be considered for periods when chorus waves are long-lasting and may influence magnetosphere-ionosphere coupling. This observation demonstrates the role of chorus waves in determining the precipitating energy spectra for the population of electrons, which contribute to ionospheric upwelling, or upflow, and preconditioning for ion outflow, as well as a successful prediction of the cutoff from theoretical predictions from equation 1.

## Acknowledgments

A.J. Halford, K. Garcia-Sage, and A. W. Breneman have been supported in part by the Goddard Internal Science Funding Model 2022 (Space Precipitation Impacts SPI). A.J. Halford was in part supported by NASA under grant numbers NNX15AF66G and NNX15AF59G, and AJH and AWB under grant NNX15AF58G. K. Garcia-Sage's effort was in part supported by the NASA Internal Scientist Funding Model (HISFM18-0006). I.R. Mann is supported by a Discovery Grant from Canadian NSERC. We acknowledge the NASA Van

Allen Probes and Harlan E. Spence and Jeff Reeves for use of the data. The ECT data can be found <http://www.rbsp-ect.lanl.gov/science/DataDirectories.php>. HOPE data was in part funded by RBSP-ECT funding provided by JHU/APL Contract No. 967399 under NASA's Prime Contract No. NAS5-01072. We would like to thank G. Hospodarsky for help with the EMFISIS data. EMFISIS data were downloaded from the Van Allen Probes EMFISIS website at <http://emfisis.physics.uiowa.edu/>. All other data used in this paper can be found on CDAweb <http://cdaweb.gsfc.nasa.gov>. We thank overleaf, github, and zenodo for making the collaboration easy on this paper. The code and data for creating the figures can be found on github [https://github.com/AJHalford/Chorus\\_Emin\\_Halford\\_et\\_al](https://github.com/AJHalford/Chorus_Emin_Halford_et_al) with the DOI: 10.5281/zenodo.3767135

## References

- Baker, D. N., Hones, E. W., Young, D. T., & Birn, J. (1982). The possible role of ionospheric oxygen in the initiation and development of plasma sheet instabilities. *Geophysical Research Letters*, 9(12), 1337–1340. Retrieved from <http://dx.doi.org/10.1029/GL009i012p01337> doi: 10.1029/GL009i012p01337
- Clemmons, J. H., Hecht, J. H., Salem, D. R., & Strickland, D. J. (2008). Thermospheric density in the earth's magnetic cusp as observed by the streak mission. *Geophysical Research Letters*, 35(24). Retrieved from <https://agupubs.onlinelibrary.wiley.com/doi/abs/10.1029/2008GL035972> doi: 10.1029/2008GL035972
- Daglis, I., Thorne, R., Baumjohann, W., & Orsini, S. (1999, Nov). The terrestrial ring current: Origin, formation, and decay. *Reviews of Geophysics*, 37, 407–438.
- Deng, Y., Fuller-Rowell, T. J., Akmaev, R. A., & Ridley, A. J. (2011). Impact of the altitudinal joule heating distribution on the thermosphere. *Journal of Geophysical Research: Space Physics*, 116(A5). Retrieved from <https://agupubs.onlinelibrary.wiley.com/doi/abs/10.1029/2010JA016019>
- Funsten, H. O., Skoug, R. M., Guthrie, A. A., MacDonald, E. A., Baldonado, J. R., Harper, R. W., ... Chen, J. (2013, March). Helium, Oxygen, Proton, and Electron (HOPE) Mass Spectrometer for the Radiation Belt Storm Probes Mission. *Space Science Reviews*. doi: 10.1007/s11214-013-9968-7
- Garcia-Sage, K., Moore, T. E., Pembroke, A., Merkin, V. G., & Hughes, W. J. (2015, October). Modeling the effects of ionospheric oxygen outflow on bursty magnetotail flows. *Journal of Geophysical Research (Space Physics)*, 120, 8723–8737. doi: 10.1002/2015JA021228
- Gkioulidou, M., Ohtani, S., Ukhorskiy, A. Y., Mitchell, D. G., Takahashi, K., Spence, H. E., ... Barnes, R. J. (2019). Low-energy (jkeV) o+ ion outflow directly into the inner magnetosphere: Van allen probes observations. *Journal of Geophysical Research: Space Physics*, 124(1), 405–419. Retrieved from <https://agupubs.onlinelibrary.wiley.com/doi/abs/10.1029/2018JA025862> doi: 10.1029/2018JA025862
- Halford, A. J. (2012). *EMIC Wave Association with Geomagnetic Storms, the Plasmasphere, and the Radiation Belts* (Unpublished doctoral dissertation). University of Newcastle Australia, Callaghan NSW Australia.
- Halford, A. J., Fraser, B. J., Morley, S. K., Elkington, S. R., & Chan, A. A. (2016). Dependence of emic wave parameters during quiet, geomagnetic storm, and geomagnetic storm phase times. *Journal of Geophysical Research: Space Physics*, 121(7), 6277–6291. Retrieved from <http://dx.doi.org/10.1002/2016JA022694> (2016JA022694) doi: 10.1002/2016JA022694
- Halford, A. J., McGregor, S. L., Hudson, M. K., Millan, R. M., & Kress, B. T. (2016). BARREL observations of a solar energetic electron and solar ener-



- getic proton event. *Journal of Geophysical Research: Space Physics*, 121(5), 4205–4216. Retrieved from <http://dx.doi.org/10.1002/2016JA022462> (2016JA022462) doi: 10.1002/2016JA022462
- Halford, A. J., McGregor, S. L., Murphy, K. R., Millan, R. M., Hudson, M. K., Woodger, L. A., ... Fennell, J. F. (2015). BARREL observations of an ICME-shock impact with the magnetosphere and the resultant radiation belt electron loss. *Journal of Geophysical Research: Space Physics*. Retrieved from <http://dx.doi.org/10.1002/2014JA020873> (2014JA020873) doi: 10.1002/2014JA020873
- Khazanov, G. V., Sibeck, D. G., & Zesta, E. (2017). Is diffuse aurora driven from above or below? *Geophysical Research Letters*, 44(2), 641–647. doi: 10.1002/2016GL072063
- Kletzing, C. A., Kurth, W. S., Acuna, M., MacDowall, R. J., Torbert, R. B., Averkamp, T., ... Tyler, J. (2013, November). The Electric and Magnetic Field Instrument Suite and Integrated Science (EMFISIS) on RBSP. *Space Science Reviews*, 179(1), 127–181.
- Li, W., Bortnik, J., Thorne, R. M., Nishimura, Y., Angelopoulos, V., & Chen, L. (2011). Modulation of whistler mode chorus waves: 2. role of density variations. *Journal of Geophysical Research: Space Physics*, 116(A6), n/a–n/a. Retrieved from <http://dx.doi.org/10.1029/2010JA016313> (A06206) doi: 10.1029/2010JA016313
- Mauk, B. H., Fox, N. J., Kanekal, S. G., Kessel, R. L., Sibeck, D. G., & Ukhorskiy, A. (2012, Sep). Science objectives and rationale for the Radiation Belt Storm Probes Mission. *Space Science Reviews*, 76. ((c) 2012: The Author(s)) doi: 10.1007/s11214-012-9908-y
- Mays, M. L., Thompson, B. J., Jian, L. K., Colaninno, R. C., Odstreil, D., Möstl, C., ... Zheng, Y. (2015, October). Propagation of the 214 January 7 CME and resulting geomagnetic non-event. *The Astrophysical Journal*, 812(2), 145.
- Meredith, N., Thorne, R., Horne, R., Summers, D., Fraser, B., & Anderson, R. (2003, Jan). Statistical analysis of relativistic electron energies for cyclotron resonance with EMIC waves observed on CRRES. *Journal of Geophysical Research*, 108. (<http://earth.agu.org/pubs/crossref/2003/2002JA009700.shtml>)
- Möstl, C., Rollett, T., Frahm, R. A., Liu, Y. D., Long, D. M., Colaninno, R. C., ... Vršnak, B. (2015, May). Strong coronal channelling and interplanetary evolution of a solar storm up to Earth and Mars. *Nature Communications*, 6, 7135.
- Ni, B., Thorne, R. M., Shprits, Y. Y., & Bortnik, J. (2008). Resonant scattering of plasma sheet electrons by whistler-mode chorus: Contribution to diffuse auroral precipitation. *Geophysical Research Letters*, 35(11), n/a–n/a. Retrieved from <http://dx.doi.org/10.1029/2008GL034032> (L11106) doi: 10.1029/2008GL034032
- Nosé, M., Oimatsu, S., Keika, K., Kletzing, C. A., Kurth, W. S., Pascuale, S. D., ... Larsen, B. A. (2015). Formation of the oxygen torus in the inner magnetosphere: Van allen probes observations. *Journal of Geophysical Research: Space Physics*, 120(2), 1182–1196. Retrieved from <https://agupubs.onlinelibrary.wiley.com/doi/abs/10.1002/2014JA020593> doi: 10.1002/2014JA020593
- Ouellette, J. E., Brambles, O. J., Lyon, J. G., Lotko, W., & Rogers, B. N. (2013). Properties of outflow-driven sawtooth substorms. *Journal of Geophysical Research: Space Physics*, 118(6), 3223–3232. Retrieved from <http://dx.doi.org/10.1002/jgra.50309> doi: 10.1002/jgra.50309
- Rae, I. J., Murphy, K. R., Watt, C. E. J., Halford, A. J., Mann, I. R., Ozeke, L. G., ... Singer, H. J. (2018). The role of localized compressional ultra-low frequency waves in energetic electron precipitation. *Journal of Geophysical Research: Space Physics*, 123(3), 1900–1914. Retrieved from <https://>

- 318 agupubs.onlinelibrary.wiley.com/doi/abs/10.1002/2017JA024674 doi:  
319 10.1002/2017JA024674
- 320 Redmon, R. J., Peterson, W. K., Andersson, L., Richards, P. G., & Yau, A. W.  
321 (2014). An assessment of the role of soft electron precipitation in global ion  
322 upwelling. *Journal of Geophysical Research: Space Physics*, 119(9), 7665–7678.  
323 Retrieved from <http://dx.doi.org/10.1002/2014JA020061> (2014JA020061)  
324 doi: 10.1002/2014JA020061
- 325 Seo, Y., Horwitz, J. L., & Caton, R. (1997). Statistical relationships between high-  
326 latitude ionospheric F region/topside upflows and their drivers: DE 2 observa-  
327 tions. *Journal of Geophysical Research*, 102, 7493. doi: 10.1029/97JA00151
- 328 Shultz, M., & Lanzerotti, L. (1974). *Particle diffusion in the radiation belt*. Springer,  
329 New York.
- 330 Spence, H. E., Reeves, G. D., Baker, D. N., Blake, J. B., Bolton, M., Bourdarie, S.,  
331 ... Thorne, R. M. (2013). Science Goals and Overview of the Radiation Belt  
332 Storm Probes (RBSP) Energetic Particle, Composition, and Thermal Plasma  
333 (ECT) Suite on NASA's Van Allen Probes Mission. *Space Science Reviews*.  
334 doi: 10.1007/978-1-4899-7433-4\_10
- 335 Su, Y.-J., Caton, R. G., Horwitz, J. L., & Richards, P. G. (1999). Systematic mod-  
336 eling of soft-electron precipitation effects on high-latitude f region and topside  
337 ionospheric upflows. *Journal of Geophysical Research: Space Physics*, 104(A1),  
338 153-163. Retrieved from [https://agupubs.onlinelibrary.wiley.com/doi/](https://agupubs.onlinelibrary.wiley.com/doi/abs/10.1029/1998JA900068)  
339 [abs/10.1029/1998JA900068](https://agupubs.onlinelibrary.wiley.com/doi/abs/10.1029/1998JA900068) doi: 10.1029/1998JA900068
- 340 Su, Z., Zheng, H., & Wang, S. (2010). A parametric study on the diffuse auroral pre-  
341 cipitation by resonant interaction with whistler mode chorus. *Journal of Geo-*  
342 *physical Research: Space Physics*, 115(A5), n/a–n/a. Retrieved from [http://](http://dx.doi.org/10.1029/2009JA014759)  
343 [dx.doi.org/10.1029/2009JA014759](http://dx.doi.org/10.1029/2009JA014759) (A05219) doi: 10.1029/2009JA014759
- 344 Summers, D., Ni, B., & Meredith, N. P. (2007). Timescales for radiation belt elec-  
345 tron acceleration and loss due to resonant wave-particle interactions: 1. The-  
346 ory. *Journal of Geophysical Research: Space Physics (1978–2012)*, 112(A4),  
347 A04206.
- 348 Zeng, W., & Horwitz, J. L. (2007). Formula representation of auroral ionospheric o+  
349 outflows based on systematic simulations with effects of soft electron precipita-  
350 tion and transverse ion heating. *Geophysical Research Letters*, 34(6), n/a–n/a.  
351 Retrieved from <http://dx.doi.org/10.1029/2006GL028632> (L06103) doi:  
352 10.1029/2006GL028632
- 353 Zhang, B., Lotko, W., Brambles, O., Wiltberger, M., Wang, W., Schmitt, P., &  
354 Lyon, J. (2012). Enhancement of thermospheric mass density by soft electron  
355 precipitation. *Geophysical Research Letters*, 39(20). Retrieved from [https://](https://agupubs.onlinelibrary.wiley.com/doi/abs/10.1029/2012GL053519)  
356 [agupubs.onlinelibrary.wiley.com/doi/abs/10.1029/2012GL053519](https://agupubs.onlinelibrary.wiley.com/doi/abs/10.1029/2012GL053519) doi:  
357 10.1029/2012GL053519



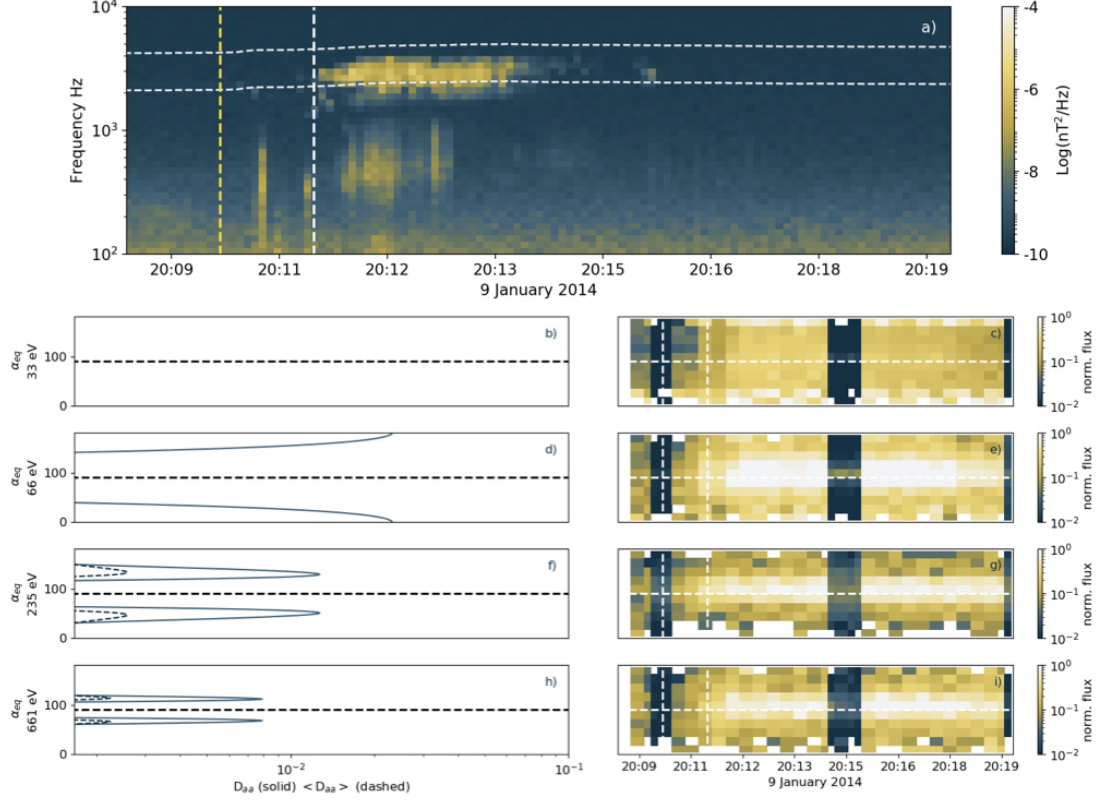


**Figure 1.** Panel a) Observations of the Chorus wave observed at Van Allen Probe B after the shock arrival on 9 January 2014. The yellow vertical line is when the iCME first encountered the magnetosphere and the white vertical line is when the chorus wave turned on. The horizontal dotted lines are the electron cyclotron frequency and 1/2 the electron cyclotron frequency. Panels b, d, f, h: The local (solid line) and the bounce averaged (dashed line) pitch angle diffusion coefficients for the Chorus wave observed for energies of approximately 33 eV, 67 eV, 235 eV, and 660 eV respectively. The x-axis corresponds to diffusion timescales less than the length of the event. Panels c, e, g, and i) The flux normalised to the peak rate in the plotted time range for the corresponding energies observed by HOPE. The horizontal yellow dotted line is at a pitch angle of 90 deg to help aid the eye.

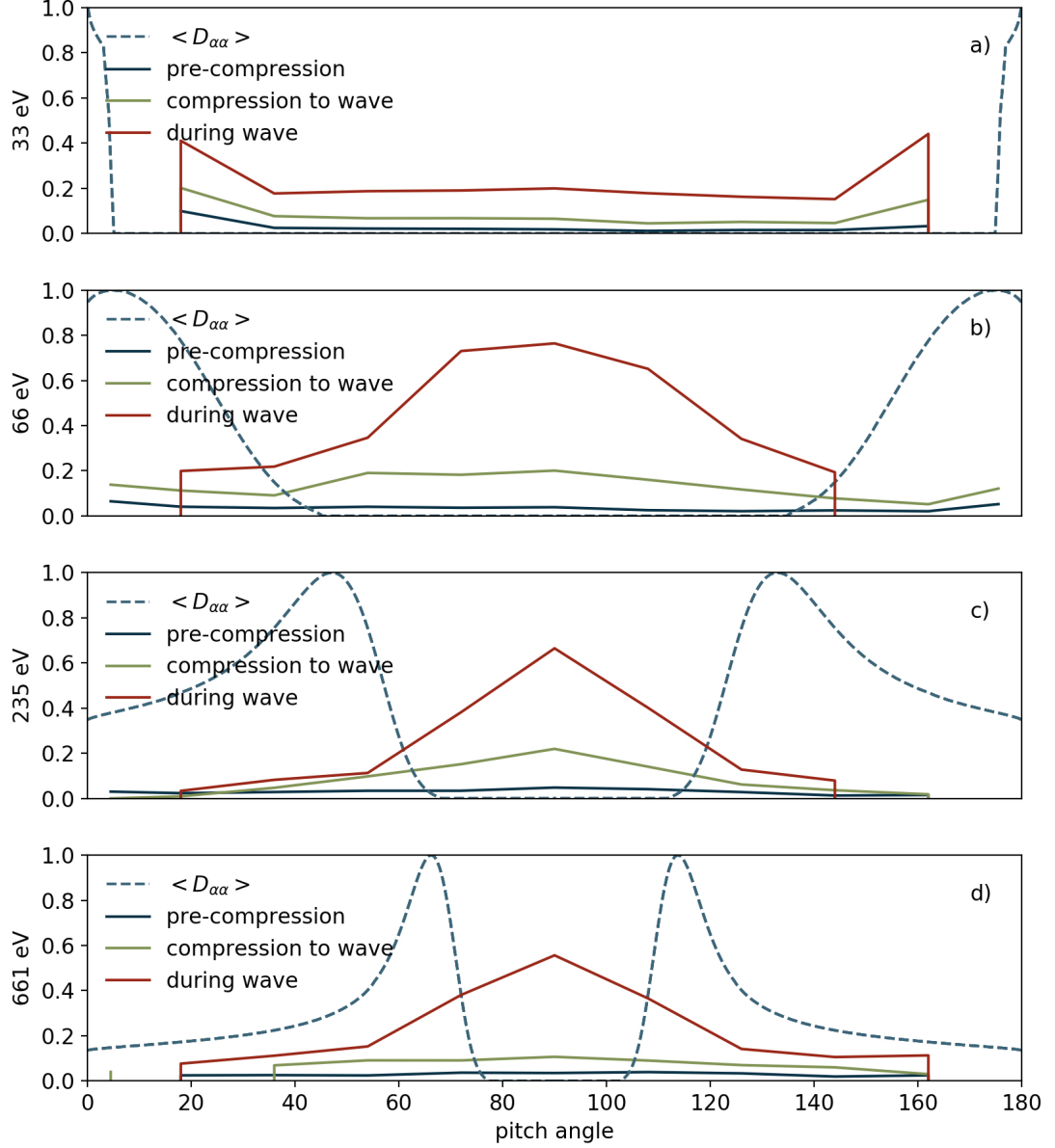


**Figure 2.** The averaged normalised pitch angle distribution for approximately 33, 66, 235, and 661 eV electrons (panels a - d) before the compression (dark blue lines), from the start of the compression till the start of the wave (green lines), and during the wave (red lines). Dashed lines show the bounce-averaged diffusion coefficients for the relevant energies.